THE JOURNAL OF PHYSICAL CHEMISTRY A
A JOURNAL OF THE AMERICAN CHEMICAL SOCIETY

pubs.acs.org/JPCA Article

Structural Characterization of 6-Thioguanosine and Its Monohydrate in the Gas Phase

Hiroyuki Saigusa,* Ayumi Oyama, Saki Kitamura, and Hiroya Asami

Cite This: *J. Phys. Chem. A* 2021, 125, 7217–7225 Read Online

ACCESS | Metrics & More | Article Recommendations | Supporting Information

ABSTRACT: Detailed structural analysis of 6-thioguanosine (6TGs) in relation to its tautomerization and sugar conformation is performed in the gas phase using UV and IR spectroscopy combined with ab initio calculations. We have observed a thiol tautomer of 6TGs with its sugar moiety in the *syn* conformation that is stabilized by a strong intramolecular H-bonding between O5′H of the sugar and N3 atom of the guanine moiety. This observation is consistent with previous results for guanosine (Gs) in which the corresponding enol form is solely detected. We have also identified a monohydrate of 6TGs consisting of a thiol tautomer with the water linking guanine moiety and sugar OH group. It is demonstrated that hydration behavior of 6TGs is significantly different from that of Gs as a result of a weaker H-bonding ability of the thiol group.

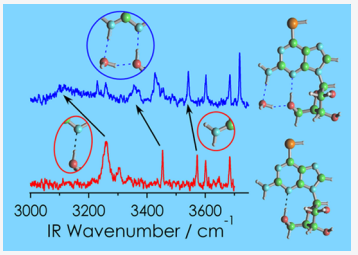

1. INTRODUCTION

6-Thioguanosine (6TGs) is a sulfur-substituted guanine nucleoside formed via N9-glysocylation of 6-thioguanine (6TG). 6TG is one of the thiopurine prodrugs and has been used as an effective anti-inflammatory, anticancer, and immunosuppressive agent.[1−4] Thiopurine prodrugs are converted into active drugs to exert their cytotoxity after metabolization and incorporation into DNA as 6TG nucleotides.[5] Later, prolonged treatment of these prodrugs was found to cause a deleterious side that the risk of acute myeloid leukemia and skin cancer increases when exposed to UVA irradiation.[6−9] Unlike canonical bases, the thioketone (thione) form of 6TG is a strong UVA chromophore with an absorbance maximum at 342 nm.[6,10] Upon UVA irradiation, it undergoes rapid intersystem crossing to the triplet state as facilitated by the presence of a heavy sulfur atom, resulting in DNA damage and cell death via the formation of reactive oxygen species. The photochemical reactivity of 6TG and 6TGs has been investigated by direct observation of singlet oxygen quantum yield and by time-resolved spectroscopy.[11−14] Though there appears to be some discrepancies in the quantum yield, these results seem to indicate that both 6TG and 6TGs are efficient reactive oxygen sensitizers.

Tautomerization preference of 6TG has been examined in various environments. X-ray crystallography indicated that 6TG exists as the thione form with a hydrogen atom bonded to the N7 site[15] and suggested that its biological functions may be related to microscopic effects that modify H-bond interactions in nucleic acids. IR studies in the argon matrix at low temperature showed that the thiol form is predominant in a hydrophobic environment,[16,17] while in polar solvents, both 6TG and 6TGs were found to be of the thione form.[18] More recently, Siouri and de Vries reported the observation of a thiol tautomer of 6TG in the gas phase using IR−UV double-resonance spectroscopy.[19] It was found that when this tautomer is electronically excited, it rapidly relaxes to a dark state, possibly a triplet, with a rate on the order of 10^{10} s^{-1}.

In contrast to 6TG, most studies of 6TGs were limited to the influence of sugar substitution on the photochemical reactivity[11−14] and its structural investigations were sparse.[18,20] In this work, detailed structural analysis of 6TGs is performed in the gas phase with emphasis on its tautomerism and sugar conformational changes. Analogous to the biologically relevant guanosine (Gs),[21] this modified nucleoside can adopt different structures due to tautomerization of the base moiety and conformational flexibility of the sugar. The most prominent tautomers are of the thione and thiol forms (Scheme 1), which correspond to the keto and enol tautomers in Gs, respectively.

Scheme 1. Three Prominent Tautomers of 6TGs[a]

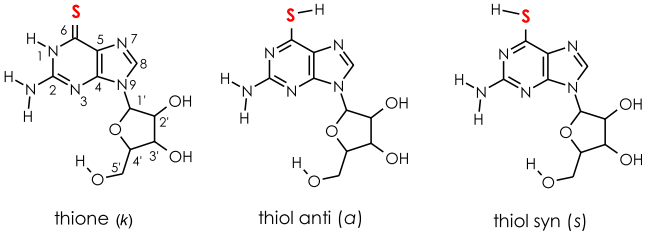

[a]The atom numbering is shown on the thione tautomer.

Received: June 13, 2021
Revised: August 3, 2021
Published: August 16, 2021

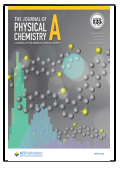

https://doi.org/10.1021/acs.jpca.1c05219
J. Phys. Chem. A 2021, 125, 7217−7225

While the presence of the sugar group prevents 7H−9H tautomerization, which is possible to occur in 6TG, it gives rise to additional conformational properties associated with N-glycosidic bond rotation and puckering motion.[22,23] We have also investigated H-bonding interactions for the monohydrated cluster of 6TGs (6TGsW) and compared with those previously reported for Gs.[24,25] Quantitative assessment of H-bonding interactions specific to sulfur-containing compounds has been carried out by Wategaonkar and co-workers.[26−30]

2. METHODS

2.1. Theoretical Calculations. Geometries of 6TGs and 6TGsW were optimized at the B3LYP/cc-pVTZ level, and subsequent single-point calculations were carried out for the lower-energy structures at the MP2/cc-pVTZ level to improve the accuracy of their energetic ordering. Harmonic vibrational frequencies and zero-point energy correction were obtained at the B3LYP/cc-pVTZ level. NBO analysis was employed to evaluate the delocalization energies from lone pair orbitals of an atom to adjacent antibonding orbitals σ^*. The delocalization energy was calculated by the second-order perturbation energy at the B3LYP/cc-pVTZ level. All calculations were performed using the Gaussian 09 quantum code package.[31]

2.2. Experimental Setup. The laser desorption technique employed in this work was described in detail elsewhere.[32] A sample pellet of 6TGs (Jena Bioscience) was prepared by mixing with a graphite matrix (10%) and irradiated by the 532 nm output of a YAG laser (Continuum Minilite I). The plume of desorbed molecules was entrained into a supersonic expansion of argon at 5 atm. Formation of hydrated clusters was achieved by mixing Ar with water vapor. Resulting jet-cooled species were ionized through resonant two-photon ionization (R2PI) using a frequency tunable UV laser (Continuum Surelite I /ND6000) and analyzed with a TOF mass spectrometer. Mass-selected UV spectra were recorded by probing ion signals at a particular mass channel while scanning UV laser frequency.

IR spectra were recorded in the region 2600−3700 cm^{-1} by the IR−UV double-resonance scheme[25,33] but not normalized with respect to the IR laser power (3−10 mJ/pulse). The UV light was operated at 10 Hz, while the IR light was generated at 5 Hz using an OPO/OPA system (LaserVision) pumped with a YAG laser (Continuum Powerlite8000). The alternate UV signals measured with the IR laser turned on (IR_{on}) and off (IR_{off}) were fed into a boxcar integrator, and their ratio was plotted as a logarithmic scale [$\log(IR_{off}/IR_{on})$].[34]

We employed an additional IR−UV double-resonance technique in which the IR laser is fixed to a specific IR transition of a particular isomer while scanning the UV laser. The resulting IR-depleted UV spectra enable us to determine whether other structural isomers are embedded in the probe UV spectra.[34,35]

3. THEORETICAL RESULTS

3.1. Low-Energy Structures of 6TGs. Figure 1 shows the low-energy structures of 6TGs optimized at the B3LYP/cc-pVTZ level. The thiol tautomer is labeled with a letter *s* or *a* to designate the rotamer with its S6 hydrogen pointing toward N1 (*syn*) or N7 (*anti*), respectively, while the thione tautomer is designated by a letter *k*. For each tautomer, there exist two major sugar conformations, *syn*−sugar and *anti*−sugar, depending on the relative orientation of base and sugar moieties with respect to the N9-glycosidic bond.[36] They are also labeled by a letter *s* or *a* following the first letter designated for the tautomerism. The *syn*−sugar conformation (Figure 1a) is more stable than the corresponding *anti*−sugar conformation (Figure 1f) as stabilized by strong internal H-bonding between O5′H of the sugar and N3 atom of the guanine moiety. In the *anti*−sugar conformation, the H-bond formed between O2′ hydrogen and N3 atoms is weaker owing to geometrical restriction of the sugar moiety.[36]

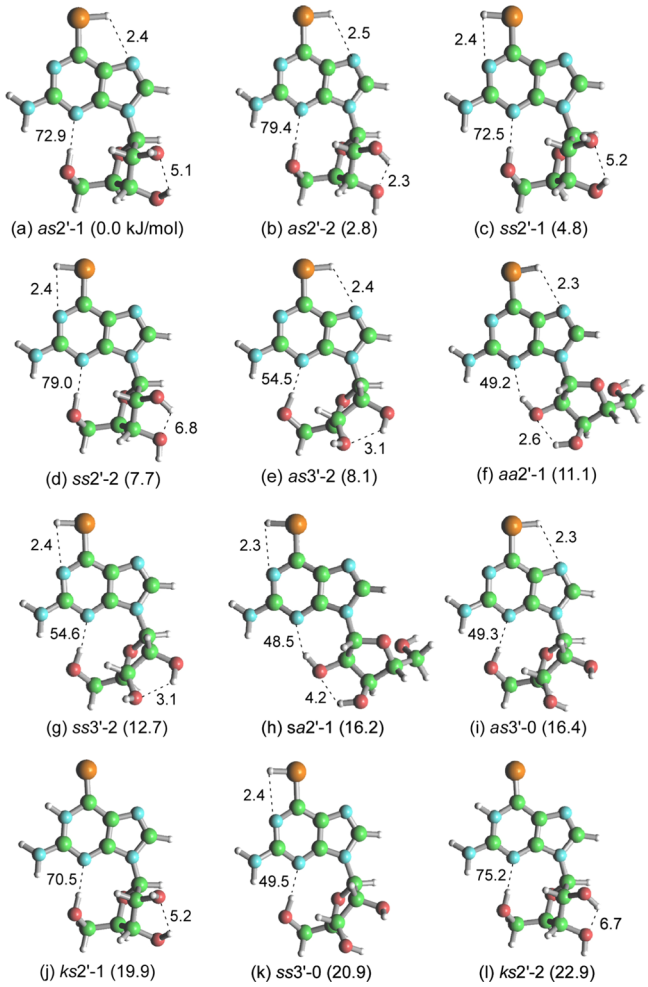

Figure 1. Low-energy structures of 6TGs optimized at the B3LYP/cc-pVTZ level. Relative energies (kJ/mol) are shown in parentheses. Broken lines indicate the formation of H-bonds derived from NBO analysis, and the interaction energies are given in kJ/mol.

There exist two additional conformations in relation to the orientation of H-bonding between O2′H and O3′H groups, analogous to the case of Gs.[21] In one, a weak H-bonding interaction occurs from O3′H to O2′, while in the other, O2′H is pointing to O3′. The former conformation is designated by a number −1 and the latter by −2. If there is no H-bond interaction between the two OH groups, it is labeled by −0 (Figure 1i,k).

It is also essential to consider conformational properties associated with puckering motions of the sugar.[22,23] Among them, C2′*endo* and C3′*endo* modes are the two most prominent conformations, which are labeled by numbers 2 and 3 with a symbol (′) as 2′ and 3′, respectively. Considering both tautomerism and sugar conformation, the *anti* rotamer

https://doi.org/10.1021/acs.jpca.1c05219
J. Phys. Chem. A 2021, 125, 7217−7225

(*a*) with *syn*−sugar (*s*) and C2′*endo* (2′) conformations (*as*2′-1) is calculated to be the most stable.

The thione tautomer is substantially higher in energy than the thiol tautomers irrespective of puckering conformations. The relative stability of the three tautomers, each having the lowest-energy sugar conformation (as2′-1, *ss*2′-1, and *ks*2′-1), is in good agreement with the previous result calculated for 9H tautomers of 6TG at the MP4(SDQ) level.[18] The instability of its thione form relative to the two thiol rotamers was accounted for by the zero-point energy (ZPE) contribution. Our calculation for 6TGs also indicates that inclusion of ZPE results in the instability of the thione form, which can be found in the Supporting Information file, Table S1. In contrast, the relative stability of the corresponding three tautomers in Gs is nearly unaffected by the ZPE correction.

Moreover, the stability of the *anti* rotamer of 6TG relative to the *syn* rotamer was ascribed to H-bond-like through-space interaction between sulfur and adjacent nitrogen atoms.[18] To reinforce this conjecture, we have performed NBO analysis on such delocalization interactions for the three tautomers of 6TGs. As summarized in Table S1, the delocalization energies of the lone pair electrons associated with the S6 atom into σ^* (N1C6 or C5C6 bond) are evaluated for 6TGs and compared with Gs. It appears that the delocalization energy calculated for the *anti* rotamer *as*2′-1 is larger by 3.3 kJ/mol than the corresponding value for the *syn* rotamer *ss*2′-1. This is in contrast to the result for Gs where the corresponding delocalization energies for the O6 atom are similar as can be seen in Table S1. Thus, both rotamers of Gs are explained to be nearly isoenergetic.

3.2. Low-Energy Structures of 6TGsW. Low-energy monohydrate structures of 6TGs are displayed in Figure 2. The

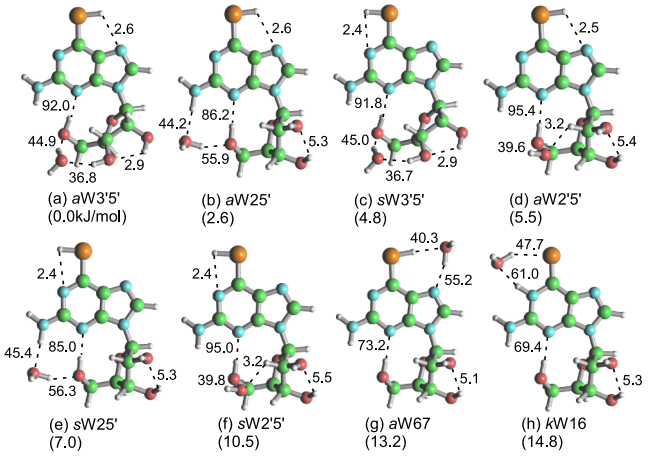

Figure 2. Low-energy structures of 6TGsW optimized at the B3LYP/cc-pVTZ level. Relative energies (kJ/mol) are shown in parenthesis. Broken lines indicate the formation of the H-bond, and the interaction energies are given in kJ/mol.

stability order appears to be rather straightforward compared to that of the bare 6TGs, and thus, we introduce a shortened notation specific to the monohydrate.[25] The most stable monohydrate shown in Figure 2a consists of the *anti* rotamer *as*3′-2 (Figure 1e) of 6TGs and the water bridging between O3′H and O5′ of the sugar, thus denoted simply as *a*W3′5′. In this case, the number −2 that denotes the direction of the H-bond between the O2′H and O3′H groups is omitted since this H-bond direction occurs only in the W3′5′ structure (Figure 2a,c). It should also be noted that the W3′5′ structures adopt C3′*endo* puckering conformation, while other hydrates are in the C2′*endo* conformation. In the monohydrate structures labeled by W2′5′ (Figure 2d,f), NBO analysis indicates that a weak H-bonding interaction is present between C2′ hydrogen and oxygen of water. Low-energy structures of GsW calculated at the present B3LYP/cc-pVTZ level are provided in the Supporting Information, Figure S1, since their stability order is in part different from that previously reported.[25]

4. EXPERIMENTAL RESULTS

4.1. UV Spectra of 6TGs and 6TGsW. Figure 3 compares the UV spectra of 6TGs and its monohydrate 6TGsW

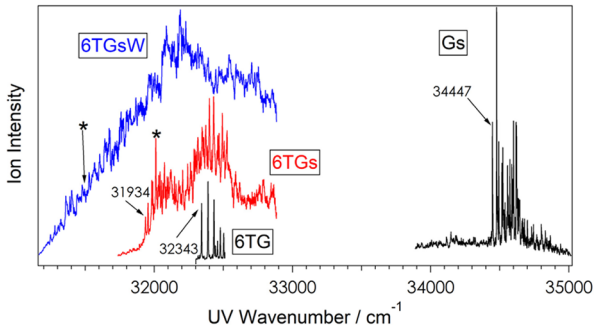

Figure 3. UV spectra of 6TGs and its monohydrate 6TGsW recorded by R2PI spectroscopy. Portions of the UV spectra reported for 6TG[19] and Gs[25] are shown for ease of comparison. Asterisks indicate the UV probe features used to record the IR spectra shown in Figure 4.

recorded by R2PI spectroscopy. The monomer spectrum consists of sharp bands with a red-most peak at 31,934 cm^{-1}. We assign this peak to the electronic origin of the UV absorption, which is red-shifted by 2513 cm^{-1} from the corresponding origin of Gs at 34,447 cm^{-1}.[21,25] The low-frequency modes above the origin are assigned to mutual motions of sugar and guanine moieties, which may be significantly affected by the electronic excitation. The origin of 6TGs is also red-shifted by 409 cm^{-1} with respect to that of 6TG at 32,343 cm^{-1} reported by Siouri et al.[19] This redshift is consistent with their assumption that the UV spectrum of 6TG is due to its 9H-thiol tautomer.

The monohydrate spectrum displayed in Figure 3 is characterized by broad absorption bands extending below 31,200 cm^{-1}. Though its UV origin is not clearly identified, the redshift from the 6TGs monomer is estimated to be >900 cm^{-1}, which indicates that 6TGs absorbs further at >320 nm by the addition of a single water molecule.

4.2. IR Spectra of 6TGs. IR spectroscopic measurements have been performed for 6TGs and 6TGsW in the IR−UV double-resonance scheme to elucidate their structural properties. The IR spectrum of 6TGs shown in the middle part of Figure 4 is recorded when probing at the prominent UV peak indicated by an asterisk in Figure 3 and compared to that of Gs (bottom) previously reported.[25] Similar IR spectra are obtained when other UV peaks appearing in Figure 3 are probed, which indicates that the UV spectrum consists of only one species. It is evident that IR spectra of Gs and 6TGs well match in the most spectral region except that the peak observed at 3587 cm^{-1} in the Gs spectrum has no corresponding peak in the 6TGs spectrum. This Gs peak is

https://doi.org/10.1021/acs.jpca.1c05219
J. Phys. Chem. A 2021, 125, 7217−7225

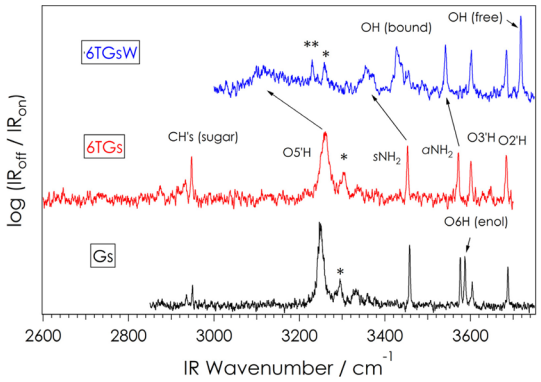

Figure 4. IR spectra of 6TGs and 6TGsW recorded by IR−UV double-resonance spectroscopy. Peaks marked by asterisks (* and **) are assigned to combination bands.

due to the enol−OH stretch of either the *syn* or *anti* rotamer.[21,25] In addition, two Gs bands that are assigned to the symmetric and antisymmetric stretches of the amino group (sNH$_2$ and aNH$_2$) are nearly unaffected by the sulfur substitution. The close resemblance of the two spectra suggests that the observed tautomer of 6TGs is of the thiol form and its sugar conformations are similar to those of Gs.

The IR spectra calculated for the three prominent tautomers of 6TGs, each having the most stable conformation, are shown in Figure 5. It is obvious that the experimental IR spectrum is

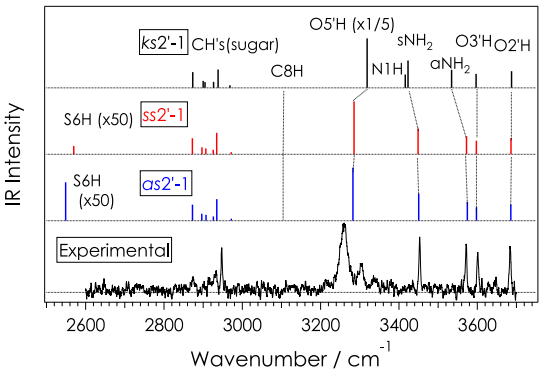

Figure 5. IR spectra (scaled by 0.959) of 6TGs calculated for three prominent tautomers having *syn*−sugar and C2′*endo*-1 conformations. The experimental IR spectrum (bottom) is taken from Figure 4.

not consistent with the thione tautomer. However, the calculated IR spectra are nearly identical for the two rotamers of the thiol form, thus yielding no unambiguous assignment of the experimental spectrum. We also observed a single rotamer for Gs and assigned to the *syn* rotamer based on the IR-frequency shift of the enol−OH stretch relative to the aNH$_2$ stretch,[25] which will be discussed later. However, in the case of 6TGs, the thiol−SH stretch shifts to a lower frequency and cannot be used as a marker band. We therefore tentatively assign the observed species to the *anti* rotamer *as*2′-1 on the basis of its relative stability to the *syn* rotamer. Experimental IR frequencies and tentative assignments for 6TGs, together with those of Gs, are listed in Table 1.

It is rather straightforward to distinguish between C2′*endo* and C3′*endo* sugar puckering conformations, as can be seen in the Supporting Information file, Figure S2. One prominent difference is that calculated IR frequencies for the O5′H

Table 1. Observed IR Frequencies (in cm^{-1}) and Tentative Assignments for 6TGs and 6TGsW[c]

Gs	6TGs	6TGsW	assignment
		3718	OH (water free)
3685	3685	3684	O2′H
3605	3602	3602	O3′H
3585			O6H (enol)
3575	3573	3542	aNH$_2$
		3426	OH (water-bound)
3455	3454	3354	sNH$_2$
3295	3304	3258	combination band *
		3229	combination band **
3251	3262	3115	O5′H
2950	2949	NA[a]	CH's (sugar)
	NA[b]	NA[a]	S6H (thiol)

[a]Not recorded. [b]Not identified. [c]Previous results obtained for Gs[25] are also shown for comparison.

stretch in the C2′*endo* conformation (Figure S2a−d) appear to be lower than those in the C3′*endo* conformation (Figure S2e), since the internal H-bond with the N3 atom is stronger in the former conformations (Figure 1a−d) than in the latter conformation (Figure 1e). Similarly, assignment of *syn*−sugar and *anti*−sugar conformations can be made in terms of the frequencies of H-bonded O5′H and O2′H stretches (Figure S2a,f).[36]

Assignment of H-bond interaction between the O2′H and O3′H groups of the sugar is problematic; the two conformers −1 and −2 give rise to similar IR spectral patterns as shown in Figure S2. Nonetheless, it was firmly established for Gs that the O3′H hydrogen points to the O2′ atom, namely, the −1 conformation, on the basis of the result for chemically modified Gs's.[21] Given the similarity of the IR spectra of Gs and 6TGs, the observed 6TGs species may be assigned to this conformer.

The IR-frequency calculation also shows that thiol SH stretching frequency shifts to around 2600 cm^{-1}, but its transition probabilities (2.9 and 0.6 km/mol for *anti* and *syn* rotamers, respectively) are two orders smaller compared to those for the CH stretching transitions of the sugar. To our knowledge, the SH stretching transitions involving the SH bonds can be observed under the jet-cooling conditions only when they are H-bonded to form molecular complexes.[26,28−30] Previous IR studies of 6TG in the argon matrix showed that complicated peaks corresponding to the SH stretching transition appear around 2605 cm^{-1} for the 9H tautomer although *syn*−*anti* rotamerism was not considered.[16,17] The corresponding transition for 6TGs in a vacuum is too weak to be detected or located below 2600 cm^{-1}.

We did not detect the thione tautomer when probing the UV spectrum of Figure 3. The failure to observe this tautomer may be explained by two reasons; it cannot be ionized effectively by the nanosecond R2PI method due to a possible ultrafast relaxation to the triplet state,[19] or its abundance in jets is low due to the relative instability. Taking account of the IR spectroscopic signatures together with the stability order, the observed 6TGs is tentatively assigned to the most stable *as*2′-1 structure or possibly the corresponding *syn* rotamer *ss*2′-1.

4.3. IR Spectra of 6TGsW. The IR spectrum of 6TGsW in Figure 4 (top) was obtained when probing at a broad feature at 31,496 cm^{-1} indicated by an asterisk in the UV absorption. We have also recorded IR spectra at several different UV features

https://doi.org/10.1021/acs.jpca.1c05219
J. Phys. Chem. A 2021, 125, 7217−7225

and found no significant difference in peak positions and the intensity pattern, which can be found in the Supporting Information, Figure S3. This suggests that the broad UV spectrum consists of only a single monohydrate, which will be discussed later.

The IR spectrum shows two sharp peaks at 3685 and 3602 cm^{-1} that can be assigned to the O2′H and O3′H stretches of the sugar, respectively. They are shifted little from the respective peaks in the bare 6TGs, and thus, it is obvious that these two sites are not occupied by H-bonding with water. In contrast, peaks corresponding to the two amino stretches and the O5′H stretch are shifted upon hydration, which indicates that these two sites are linked by the water. Among the low-energy monohydrate structures shown in Figure 2, both *a*W25′ and *s*W25′ structures are consistent with this observation. Experimental IR frequencies and tentative assignments for 6TGsW are listed in Table 1.

Figure 6 shows the IR spectra calculated for the two most stable structures *a*W3′5′ and *a*W25′ displayed in Figure 2,

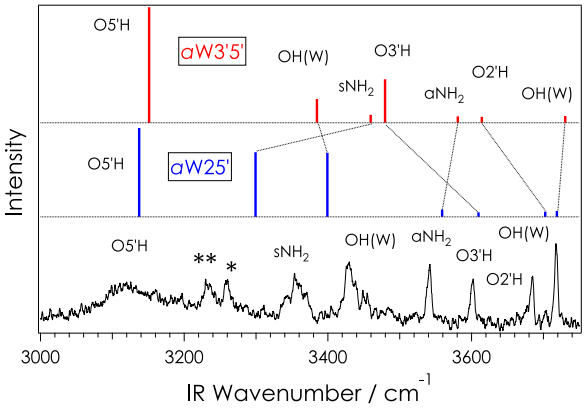

Figure 6. IR spectra (scaled by 0.963) calculated for the two most stable structures *a*W3′5′ and *a*W25′ displayed in Figure 2. The experimental IR spectrum (bottom) is taken from Figure 4.

which is compared with the experimental spectrum taken from Figure 4. Corresponding IR spectra for the *syn* rotamers *s*W3′5′ and *s*W25′ are nearly the same as those of the *anti* rotamers, which are shown in the Supporting Information, Figure S4. While the observed spectrum agrees well with both monohydrates *a*W25′ and *s*W25′ (Figure 2b,e), we tentatively assign the observed monohydrate to the *a*W25′ on the basis of its relative stability of 4.4 kJ/mol with respect to the *s*W25′.

It has been documented that amino−keto forms of 9H-guanine and other 9-substituted guanines cannot be detected by nanosecond R2PI spectroscopy due to short excited-state lifetimes.[37,38] Nevertheless, we were able to observe the monohydrates of the keto tautomer *k*W16 in 9-methylguanine (9MG) and Gs by the same spectroscopic technique.[25] The results seem to suggest that the ultrafast deactivation process is suppressed when H-bonding takes place to form a cyclic structure N1H−W−O6C. In this study, we have not observed the corresponding monohydrate of the thione form, which may be ascribed to the less stability with respect to the thiol monohydrates.

There are two additional peaks marked by asterisks that cannot be readily assigned to the calculated fundamental vibrations. They appear to be blue-shifted approximately by 114 and 143 cm^{-1} with respect to the center of the broad O5′H band. One possible assignment is that they correspond to mutual motions of sugar and guanine moieties, which may be coupled with O5′H stretch through intramolecular H-bonding interaction.

So far, we have identified only one monohydrate of 6TGs in which the water molecule links amino hydrogen and O5′ atom of the sugar to form a cyclic structure W25′. To determine whether other low-energy monohydrates such as W3′5′ are present in the probe UV spectrum, we have employed the technique of IR-depleted UV spectroscopy.[34,35,40] The vibrational frequency calculation shown in Figure S4 indicates that the amino stretching frequencies of the W3′5′ monohydrate are not significantly influenced by the addition of water. Therefore, the IR laser is fixed at the well-isolated peak assigned to the water-bound aNH_2 stretch at 3542 cm^{-1}, and the UV laser is scanned with an alternate IR laser on and off. With this IR irradiation, only species having a W25′ structure will be depopulated, while the monohydrate of W3′5′, if exists, survives.

The resulting IR-depleted UV spectra are shown in Figure 7. The two spectra recorded with IR on and IR off are apparently

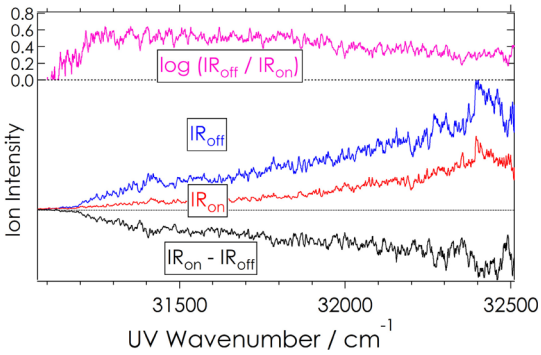

Figure 7. IR-depleted UV spectra recorded by fixing IR laser frequency to the peak at 3542 cm^{-1} of the W25′monohydrate shown in Figure 4 (top). Spectra shown in red and blue are obtained with an IR laser on (IR_{on}) and off (IR_{off}), respectively, while the difference spectrum $IR_{on}-IR_{off}$ is shown in black. IR-depletion yield $\log(IR_{off}/IR_{on})$ plotted as a function of UV frequency is shown in the top panel.

similar in the intensity distribution, which suggests that the entire UV spectrum consists only of the monohydrate structure W25′. To see this more clearly, IR-depletion yield of the UV intensity defined as $\log(IR_{off}/IR_{on})$ is plotted as a function of the UV frequency as in the top panel of Figure 7. The signal appears to be nearly constant with values of 0.5, firmly supporting that monohydrates having free NH_2 stretches (W3′5′) are not present in this range. Close examination of the curve reveals that the depletion yield slightly decreases at frequencies above 32,000 cm^{-1}. Nonetheless, we have not obtained clear evidence for peaks assignable to free NH_2 stretches when IR spectra are recorded in this region (Figure S3). Considering this result, we have concluded that there exists only a single monohydrate, either *a*W25′or *s*W25′ in the UV spectrum.

5. DISCUSSION

5.1. Observation of a Single Thiol Rotamer. The present results show that we observe a single rotamer of the thiol form for 6TGs, which is consistent with the result reported for 6TG by Siouri et al.[19] They also detected only a thiol tautomer by employing both nano- and picosecond R2PI

https://doi.org/10.1021/acs.jpca.1c05219
J. Phys. Chem. A 2021, 125, 7217−7225

techniques and suggested that this tautomer, assumed as the *syn* rotamer, undergoes a picosecond decay to a dark state, possibly a triplet state.[19] Therefore, it is intriguing to examine whether *syn* and *anti* rotamers show distinct excited-state dynamics. One possible cause of such a rotamer-specific ultrafast relaxation is related to the location of an nπ^* excited state associated with the thiol group relative to the initially excited $\pi\pi^*$ state. Previous CNDO/S calculation results on the excite-state energies of 9H−6TG suggested that for the *anti* rotamer, a singlet nπ^* state is located in the vicinity of the $\pi\pi^*$ excited state.[18] However, a more recent calculation for the *syn* rotamer of 9H-6TG showed that the corresponding nπ^* state is higher in energy by 0.51 eV than the $\pi\pi^*$ state.[19] This calculation also indicated the existence of an nπ^* triplet state in close proximity to the initially excited $\pi\pi^*$state. In the case of S6-methylthioinosine in which its S6-methyl group points toward N1 (*syn*) or N7 (*anti*), the singlet nπ^* state is calculated to be nearly isoenergetic to the $\pi\pi^*$ state for both rotamers in a vacuum.[14]

The results obtained for 6TG and 6TGs parallel those of the 9H-enol form of bare guanine[39−41] and 9MG[25,41] where nanosecond lasers were utilized for R2PI. For 9MG, Chin et al. assigned the observed rotamer to the *anti*−enol form based on comparison with the result for the monohydrate[42] and suggested a strong coupling of the initially excited $\pi\pi^*$state with a low-lying nπ^* state for this rotamer.[40] In our previous study of Gs, the IR spectrum shown in Figure 4 (bottom) was assigned to the *syn* rotamer,[25] since the enol−OH stretch frequency is calculated to be slightly lower than that of the O3′H stretch while vice versa in the *anti* rotamer, as shown in the Supporting Information file, Figure S5. In contrast, both *syn* and *anti* rotamers were observed for 9H-enol guanine when IR spectra were recorded in helium droplets.[43]

Another intriguing explanation for the observation of a specific rotamer in the 9H-enol guanine was provided by Marian;[44] the *syn* rotamer of 9H-guanine rapidly relaxes to the ground state via a conical intersection, whereas the *anti* rotamer gives rise to no such dynamics. Chen and Li calculated the excited-state geometry only for the *anti* rotamer and suggested that such ultrafast dynamics are less likely to occur in this rotamer.[45] However, it is uncertain whether similar rotamer-dependent excited-state dynamics are possible in the case of 6TGs, thus requiring a high-level computational treatment in order to corroborate the experimental findings.

5.2. Hydration Preference of 6TGs. The relative energies of 6TGsW shown in Figure 2 are schematically displayed in Figure 8 and compared with those of GsW (Figure S1). It is evident that the stabilization energies of 6TGsW spread over a wider energy range than those of GsW. This difference is largely attributed to the stability order of the three tautomers in 6TGs, which is *anti* > *syn* ≫ thione as opposed to the case of three nearly isoenegetic tautomers in Gs.

In addition, the *a*W67 structure of 6TGsW is calculated to be unstable, while the corresponding monohydrate of Gs is the most stable.[25] The larger stability of the Gs hydrate is ascribed to a strong H-bonding interaction between O6 hydrogen and oxygen of water (101.7 kJ/mol, Figure S1a). The corresponding interaction in the *a*W67 structure of 6TGs (Figure 2g) is calculated to be only 40.3 kJ/mol, thus explaining the instability of 13.2 kJ/mol with respect to the most stable one.

As shown in Figure 2, monohydrates of the thione tautomer are less stable than those of the thiol tautomers. The lowest-energy monohydrate of the thione form corresponds to the

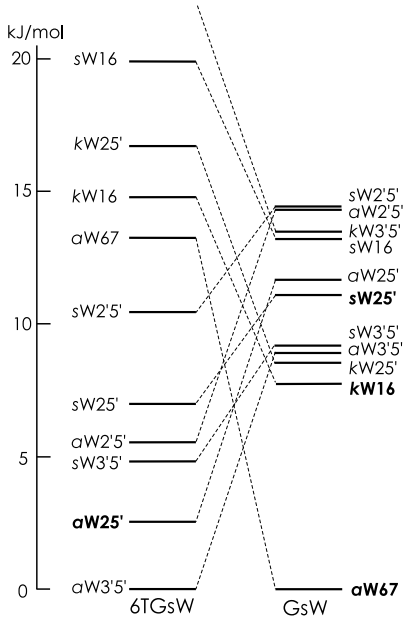

Figure 8. Schematic energy diagram compared for 6TGsW and GsW. The energy of the most stable monohydrate is taken as the baseline. Experimentally identified structures are highlighted in bold, with the ambiguity of *syn* or *anti* rotamers for the monohydrates of W25′. Relative stabilities and optimized structures for GsW calculated at the B3LYP/cc-pVTZ level are shown in Figure S1.

*k*W16 structure (Figure 2h), which is less stable by 14.8 kJ/mol than that of the most stable *a*W3′5′ structure. NBO analysis indicates that H-bond energies calculated for the *k*W16 structure are not significantly different for 6TGsW (Figure 2h) and GsW (Figure S1b). Therefore, the instability of the thione monohydrate *k*W16 can be ascribed to that of the monomer shown in Figure 1j.

5.3. Search for the Calculated Most Stable Monohydrate. We have identified only a single monohydrate, either *a*W25′ or *s*W25′, in which NH_2 hydrogen of the base and the O5′atom of the sugar are linked by water. In the case of GsW, the corresponding monohydrate was observed in addition to two other monohydrates, each with water H-bonded to enol−OH (*a*W67, Figure S1a) or H-bonded to C6O of the keto tautomer (*k*W16, Figure S1b).[25] The latter two monohydrates are less stable in 6TGsW as a consequence of weak H-bonding interaction of the S6H bond relative to the O6H bond. Therefore, hydration tends to occur around the sugar moiety as discussed above.

The apparent failure to observe the calculated most stable monohydrate *a*W3′5′ is somewhat a puzzle. In this monohydrate structure, H-bonding network O2′H−O3′H−W−O5′H−N3 is formed upon hydration, which reinforces the internal H-bond between the O5′H and N3 atoms as shown in Figure 2a. Thus, its UV spectrum is expected to appear in the lower spectral region than that of the bare 6TGs in Figure 3. Nevertheless, we have obtained no evidence for the W3′5′ monohydrates in the IR-depleted UV spectrum of Figure 7, which is consistent with our previous result for GsW.[25] We have also examined the possibility of extensive fragmentation of this monohydrate upon photoionization and found no spectral features assignable to such monohydrates in the UV spectrum when probed at the monomer mass channel.

The monohydrates of the W3′5′ structure adopt C3′*endo* conformation as shown in Figure 2, while the most stable

https://doi.org/10.1021/acs.jpca.1c05219
J. Phys. Chem. A 2021, 125, 7217−7225

monomer possesses C2′*endo* conformation. This leads us to speculate that monomers having C2′*endo* conformation are prevalent upon laser desorption and jet-cooling, and subsequent microhydration occurs around the low-temperature monomers where conformational changes of the sugar are no longer possible. A similar hydration behavior, referred to as "memory effect," was proposed for the monohydrate distribution of model peptides produced by laser desorption.[46] Analysis of X-ray crystallography showed that 6TGs exists in the C2′*endo* conformation in the crystal structure.[20,47,48] The barrier height between C2′*endo* and C3′*endo* conformers is not known for 6TGs, but the corresponding value for Gs is estimated to be 20 kJ/mol.[49−51]

In order to ascertain whether such a memory effect is consistent with the present observation, we have examined temperature dependence of Gibbs free energy[46] for the two stable monohydrates *a*W3′5′ and *a*W25′. The result obtained at the B3LYP/cc-pVTZ level is shown in Figure 9. It appears

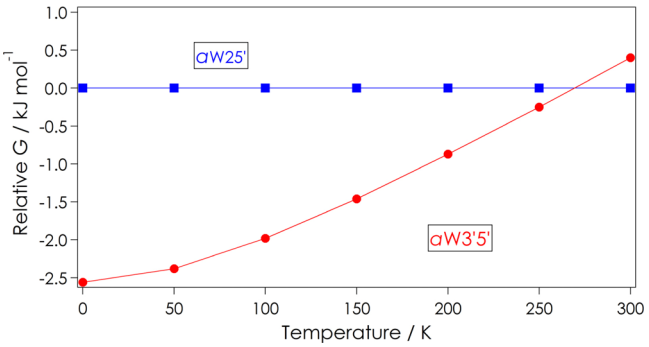

Figure 9. Temperature dependence of relative Gibbs free energies (in kJ/mol^{-1}) calculated at the B3LYP/cc-pVTZ level for the monohydrates of *a*W3′5′ and *a*W25′ structures. The energies are relative to those of the observed *a*W25′ monohydrate.

that the relative Gibbs free energy of the *a*W3′5′ monohydrate with respect to the *a*W25′ monohydrate increases with temperature and the latter monohydrate is more stable at >270 K. If the final distribution were governed by a thermal equilibrium at low temperature, the *a*W3′5′ monohydrate would be stabilized by the formation of a H-bonding network. If on the other hand, the hydrate distribution is governed by the relative stability associated with the C2′ *endo* conformation, the *a*W25′ monohydrate will be abundant, irrespective of its relative instability at <270 K.

To conclude this section, it is suggested that the relative abundance of 6TGsW is controlled by the stability of sugar puckering conformations of 6TGs, to account for the absence of the calculated most stable W3′5′ monohydrate. Apparently, more detailed considerations of how the conformer stabilization and hydration take place during the jet-cooling process are required to elaborate this interpretation.

6. CONCLUSIONS

Detailed structural analysis of 6TGs and its monohydrate has been performed using UV and IR spectroscopy combined with ab initio calculations. For bare 6TGs, we have observed a single tautomer assignable to the thiol form with its SH group either in the *anti* or possibly *syn* rotameric direction. This observation is similar to the previous result for Gs in which only an enol tautomer was detected. We have also identified a monohydrate and assigned to a thiol tautomer with water linking guanine and sugar moieties to form a cyclic structure. This hydration behavior is significantly different from the case of Gs where three stable structures are found to coexist. The hydrophobic nature of 6TGs with respect to Gs is rationalized by the weak H-bonding ability of the thiol SH group. Neither the thione tautomer of 6TGs nor its monohydrate has been observed, which can be interpreted either by the possibility of short excited-state lifetimes or by their instability with respect to the thiol form. Taking account of the present structural analyses of 6TGs and its monohydrate, it would be worthwhile elucidating their rotamer-specific excited-state dynamics in comparison with those of Gs.

■ ASSOCIATED CONTENT

Supporting Information

The Supporting Information is available free of charge at https://pubs.acs.org/doi/10.1021/acs.jpca.1c05219.

Relative energies and optimized structures of GsW; IR spectra calculated for the three tautomers of Gs; IR spectra calculated for the low-energy structures of 6TGs; IR spectra of 6TGsW recorded at different UV probe frequencies; IR spectra calculated for the eight most stable monohydrates of 6TGs; calculated energies, relative energies, and delocalization energies for three tautomers of 6TGs in comparison with those for Gs (PDF)

■ AUTHOR INFORMATION

Corresponding Author

Hiroyuki Saigusa − *Graduate School for Bio- and Nanosystem Sciences, Yokohama City University, Yokohama 236-0027, Japan;* orcid.org/0000-0001-8692-7197; Email: saigusa@yokohama-cu.ac.jp

Authors

Ayumi Oyama − *Graduate School for Bio- and Nanosystem Sciences, Yokohama City University, Yokohama 236-0027, Japan*

Saki Kitamura − *Graduate School for Bio- and Nanosystem Sciences, Yokohama City University, Yokohama 236-0027, Japan*

Hiroya Asami − *Department of Chemistry, Faculty of Science, Gakushuin University, Tokyo 171-8588, Japan*

Complete contact information is available at: https://pubs.acs.org/10.1021/acs.jpca.1c05219

Notes

The authors declare no competing financial interest.

■ ACKNOWLEDGMENTS

This work was supported in part by the Grant−in−Aid from JSPS (16 K05662).

■ REFERENCES

(1) Elion, G. B. The Purine Path to Chemotherapy. *Science* **1989**, *244*, 41−47.

(2) Quantitation of 6-Thioguanine Residues in Peripheral Blood Leukocyte DNA Obtained from Patients Receiving 6-Mercaptopurine-based Maintenance Therapy. *Cancer Res.* **1995**, *55*, 1670−1674.

(3) Relling, M. V.; Dervieux, T. Pharmacogenetics and Cancer Therapy. *Nat. Rev. Cancer* **2001**, *1*, 99−108.

(4) Cuffari, C.; Li, D. Y.; Mahoney, J.; Barnes, Y.; Bayless, T. M. Peripheral Blood Mononuclear Cell DNA 6-Thioguanine Metabolite

Levels Correlate with Decreased Interferon-Gamma Production in Patients with Crohn's Disease on Aza Therapy. *Dig. Dis. Sci.* **2004**, *49*, 133−137.
(5) Karran, P.; Attard, N. Thiopurines in Current Medical Practice: Molecular Mechanisms and Contributions to Therapy-Related Cancer. *Nat. Rev. Cancer* **2008**, *8*, 24−36.
(6) Aarbakke, J.; Janka-Schaub, G.; Elion, G. B. Thiopurine biology and pharmacology. *Trends Pharmacol. Sci.* **1997**, *18*, 3−7.
(7) O'Donovan, P.; Perrett, C. M.; Zhang, X.; Montaner, B.; Xu, Y.-Z.; Harwood, C. A.; McGregor, J. M.; Walker, S. L.; Hanaoka, F.; Karran, P. Azathioprine and UVA Light Generate Mutagenic Oxidative DNA Damage. *Science* **2005**, *309*, 1871−1874.
(8) Zhang, X.; Jeffs, G.; Ren, X.; O'Donovan, P.; Montaner, B.; Perrett, C. M.; Karran, P.; Xu, Y.-Z. Novel DNA Lesions Generated by the Interaction Between Therapeutic Thiopurines and UVA Light. *DNA Repair* **2007**, *6*, 344−354.
(9) Montaner, B.; O'Donovan, P.; Reelfs, O.; Perrett, C. M.; Zhang, X.; Xu, Y. Z.; Ren, X.; Macpherson, P.; Frith, D.; Karran, P. Reactive Oxygen-Mediated Damage to a Human DNA Replication and Repair Protein. *EMBO Rep.* **2007**, *8*, 1074−1079.
(10) Brem, R.; Guven, M.; Karran, P. Oxidatively-Generated Damage to DNA and Proteins Mediated by Photosensitized UVA. *Free Radical Biol. Med.* **2017**, *107*, 101−109.
(11) Zhang, Y.; Zhu, X.; Smith, J.; Haygood, M. T.; Gao, R. Direct Observation and Quantitative Characterization of Singlet Oxygen in Aqueous Solution upon UVA Excitation of 6-Thioguanines. *J. Phys. Chem. B* **2011**, *115*, 1889−1894.
(12) Reichardt, C.; Guo, C.; Crespo-Hernández, C. E. Excited-State Dynamics in 6-Thioguanosine from the Femtosecond to Microsecond Time Scale. *J. Phys. Chem. B* **2011**, *115*, 3263−3270.
(13) Ashwood, B.; Jockusch, S.; Crespo-Hernández, C. Excited-State Dynamics of the Thiopurine Prodrug 6-Thioguanine: Can N9-Glycosylation Affect Its Phototoxic Activity? *Molecules* **2017**, *22*, 379.
(14) Ashwood, B.; Ortiz-Rodríguez, L. A.; Crespo-Hernández, C. E. Photochemical Relaxation Pathways of S6-Methylthioinosine and O6-Methylguanosine in Solution. *Faraday Discuss.* **2018**, *207*, 351−374.
(15) Bugg, C. E.; Thewalt, U. The Crystal and Molecular Structure of 6-Thioguanine. *J. Am. Chem. Soc.* **1970**, *92*, 7441−7445.
(16) Szczepaniak, K.; Person, W. B.; Leszczyński, J.; Kwiatkowski, J. S. Tautomerism of Thioguanine. Experimental Matrix Isolation and Theoretical Quantum-Mechanical Studies. *Postepy Biochem.* **1995**, *41*, 300−308.
(17) Kasende, O. E. Infrared Spectra of 6-Thioguanine Tautomers. An Experimental and Theoretical Approach. *Spectrochim. Acta, Part A* **2002**, *58*, 1793−1808.
(18) Stewart, M. J.; Leszczynski, J.; Rubin, Y. V.; Blagoi, Y. P. Tautomerism of Thioguanine: From Gas Phase to DNA. *J. Phys. Chem. A* **1997**, *101*, 4753−4760.
(19) Siouri, F. M.; Boldissar, S.; Berenbeim, J. A.; de Vries, M. S. Excited State Dynamics of 6-Thioguanine. *J. Phys. Chem. A* **2017**, *121*, 5257−5266.
(20) Thewalt, U.; Bugg, C. E. Effects of sulfur substituents on base stacking and hydrogen bonding. Crystal structure of 6-thioguanosine monohydrate. *J. Am. Chem. Soc.* **1972**, *94*, 8892−8898.
(21) Nir, E.; Hünig, I.; Kleinermanns, K.; de Vries, M. S. Conformers of Guanosines and their Vibrations in the Electronic Ground and Excited States, as Revealed by Double-Resonance Spectroscopy and Ab Initio Calculations. *ChemPhysChem* **2004**, *5*, 131−137.
(22) Saenger, W. *Principles of Nucleic Acid Structure*. Springer-Verlag: New York, 1984.
(23) Altona, C.; Sundaralingam, M. Conformational Analysis of the Sugar Ring in Nucleosides and Nucleotides. A New Description Using the Concept of Pseudorotation. *J. Am. Chem. Soc.* **1972**, *94*, 8205−8212.
(24) Saigusa, H.; Mizuno, N.; Asami, H.; Takahashi, K.; Tachikawa, M. Ultraviolet Spectroscopy and Theoretical Calculations of Mono- and Dihydrated Clusters of the Guanine Nucleosides: Possibility of Different Hydration Structures for Guanosine and 2′-Deoxyguanosine. *Bull. Chem. Soc. Jpn.* **2008**, *81*, 1274−1281.
(25) Saigusa, H.; Urashima, S.; Asami, H. IR-UV Double Resonance Spectroscopy of the Hydrated Clusters of Guanosine and 9-Methylguanine: Evidence for Hydration Structures Involving the Sugar Group. *J. Phys. Chem. A.* **2009**, *113*, 3455−3462.
(26) Biswal, H. S.; Wategaonkar, S. Sulfur, Not Too Far Behind O, N, and C: SH···π Hydrogen Bond. *J. Phys. Chem. A* **2009**, *113*, 12774−12782.
(27) Biswal, H. S.; Shirhatti, P. R.; Wategaonkar, S. O−H···O versus O−H···S Hydrogen Bonding. 2. Alcohols and Thiols as Hydrogen Bond Acceptors. *J. Phys. Chem. A* **2010**, *114*, 6944−6955.
(28) Bhattacherjee, A.; Matsuda, Y.; Fujii, A.; Wategaonkar, S. The Intermolecular S−H···Y (Y=S,O) Hydrogen Bond in the H_2S Dimer and the H_2S−MeOH Complex. *ChemPhysChem* **2013**, *14*, 905−914.
(29) Bhattacherjee, A.; Matsuda, Y.; Fujii, A.; Wategaonkar, S. Acid−Base Formalism in Dispersion-Stabilized S−H···Y (Y=O, S) Hydrogen-Bonding Interactions. *J. Phys. Chem. A* **2015**, *119*, 1117−1126.
(30) Biswal, H. S.; Bhattacharyya, S.; Bhattacherjee, A.; Wategaonkar, S. Nature and Strength of Sulfur-Centred Hydrogen Bonds: Laser Spectroscopic Investigations in the Gas Phase and Quantum-Chemical Calculations. *Int. Rev. Phys. Chem.* **2015**, *34*, 99−160.
(31) Frisch, M. J.; Trucks, G. W.; Schlegel, H. B.; Scuseria, G. E.; Robb, M. A.; Cheeseman, J. R.; Scalmani, G.; Barone, V.; Mennucci, B.; Petersson, G. A.; et al. *Gaussian 09 Revision A.02*. Gaussian, Inc.: Wallingford, CT, 2009.
(32) Saigusa, H. Excited-State Dynamics of Isolated Nucleic Acid Bases and Their Clusters. *J. Photochem. Photobiol. C* **2006**, *7*, 197−210.
(33) Asami, H.; Saigusa, H. Multiple Hydrogen-Bonding Interactions of Uric Acid/9-Methyluric Acid with Melamine Identified by Infrared Spectroscopy. *J. Phys. Chem. B* **2014**, *118*, 4851−4857.
(34) Asami, H.; Urashima, S.; Saigusa, H. Structural Identification of Uric Acid and Its Monohydrates by IR−UV Double Resonance Spectroscopy. *Phys. Chem. Chem. Phys.* **2011**, *13*, 20476−20480.
(35) Saigusa, H.; Nakamura, D.; Urashima, S. Hydrogen-Bonding Interactions of Uric Acid Complexes with Water/Melamine by Mid-Infrared Spectroscopy. *Phys. Chem. Chem. Phys.* **2015**, *17*, 23026−23033.
(36) Asami, H.; Urashima, S.; Tsukamoto, M.; Motoda, A.; Hayakawa, Y.; Saigusa, H. Controlling Glycosyl Bond Conformation of Guanine Nucleosides: Stabilization of the anti Conformer in 5′-O-Ethylguanosine. *J. Phys. Chem. Lett.* **2012**, *3*, 571−575.
(37) Mons, M.; Piuzzi, F.; Dimicoli, I.; Gorb, L.; Leszczynski, J. Near-UV Resonant Two-Photon Ionization Spectroscopy of Gas Phase Guanine: Evidence for the Observation of Three Rare Tautomers. *J. Phys. Chem. A* **2006**, *110*, 10921−10924.
(38) Asami, H.; Tokugawa, M.; Masaki, Y.; Ishiuchi, S.; Gloaguen, E.; Seio, K.; Saigusa, H.; Fujii, M.; Sekine, M.; Mons, M. Effective Strategy for Conformer-Selective Detection of Short-Lived Excited State Species: Application to the IR Spectroscopy of the N1H Keto Tautomer of Guanine. *J. Phys. Chem. A* **2016**, *120*, 2179−2184.
(39) Nir, E.; Janzen, C.; Imhof, P.; Kleinermanns, K.; de Vries, M. S. Guanine Tautomerism Revealed by UV−UV and IR−UV Hole Burning Spectroscopy. *J. Chem. Phys.* **2001**, *115*, 4604−4611.
(40) Chin, W.; Mons, M.; Dimicoli, I.; Piuzzi, F.; Tardivel, B.; Elhanine, M. Tautomer Contributions to the Near UV Spectrum of Guanine: Towards a Refined Picture for the Spectroscopy of Purine Molecules. *Eur. Phys. J. D* **2002**, *20*, 347−355.
(41) Mons, M.; Dimicoli, I.; Piuzzi, F.; Tardivel, B.; Elhanine, M. Tautomerism of the DNA Base Guanine and Its Methylated Derivatives as Studied by Gas-Phase Infrared and Ultraviolet Spectroscopy. *J. Phys. Chem. A* **2002**, *106*, 5088−5094.
(42) Chin, W.; Mons, M.; Piuzzi, F.; Tardivel, B.; Dimicoli, I.; Gorb, L.; Leszczynski, J. Gas Phase Rotamers of the Nucleobase 9-Methylguanine Enol and Its Monohydrate: Optical Spectroscopy and

https://doi.org/10.1021/acs.jpca.1c05219
J. Phys. Chem. A 2021, 125, 7217−7225

Quantum Mechanical Calculations. *J. Phys. Chem. A* **2004**, *108*, 8237−8243.
(43) Choi, M. Y.; Miller, R. E. Four Tautomers of Isolated Guanine from Infrared Laser Spectroscopy in Helium Nanodroplets. *J. Am. Chem. Soc.* **2006**, *128*, 7320−7328.
(44) Marian, C. M. The Guanine Tautomer Puzzle: Quantum Chemical Investigation of Ground and Excited States. *J. Phys. Chem. A* **2007**, *111*, 1545−1553.
(45) Chen, H.; Li, S. Theoretical Study on the Excitation Energies of Six Tautomers of Guanine: Evidence for the Assignment of the Rare Tautomers. *J. Phys. Chem. A* **2006**, *110*, 12360−12362.
(46) Biswal, H. S.; Loquais, Y.; Tardivel, B.; Gloaguen, E.; Mons, M. Isolated Monohydrates of a Model Peptide Chain: Effect of a First Water Molecule on the Secondary Structure of a Capped Phenylalanine. *J. Am. Chem. Soc.* **2011**, *133*, 3931−3942.
(47) The Crystal Structure of Guanosine Dihydrate and Inosine Dihydrate. *Acta Cryst. B* **1970**, *26*, 1089−1101, DOI: 10.1107/S0567740870003667.
(48) Mande, S. S.; Seshadri, T. P.; Viswamitra, M. A. Structure of S-(p-Nitrobenzyl)-6-Thioguanosine. *Curr. Sci.* **1988**, *57*, 923−925.
(49) Roder, O.; Ludemann, H.-D.; von Goldammer, E. Determination of the Activation Energy for Pseudorotation of the Furanose Ring in Nucleosides by ^{13}C Nuclear-Magnetic-Resonance Relaxation. *Eur. J. Biochem.* **1975**, *53*, 517−524.
(50) Brameld, K. A.; Goddard, W. A. Ab Initio Quantum Mechanical Study of the Structures and Energies for the Pseudorotation of 5'-Dehydroxy Analogues of 2'-Deoxyribose and Ribose Sugars. *J. Am. Chem. Soc.* **1999**, *121*, 985−993.
(51) Huang, H.; Giese, T. J.; Lee, T. -S.; York, D. M. Improvement of DNA and RNA Sugar Pucker Profiles from Semiempirical Quantum Methods. *J. Chem. Theory Comput.* **2014**, *10*, 1538−1545.

https://doi.org/10.1021/acs.jpca.1c05219
J. Phys. Chem. A 2021, 125, 7217−7225